

See discussions, stats, and author profiles for this publication at: <https://www.researchgate.net/publication/258798423>

Estimation of the elasto-plastic properties of metallic materials from micro-hardness measurements

Article in *Journal of Materials Science* · June 2013

DOI: 10.1007/s10853-013-7263-3

CITATIONS

3

READS

42

3 authors:



Chunyu Zhang

Sun Yat-Sen University

26 PUBLICATIONS 217 CITATIONS

[SEE PROFILE](#)



Faxin Li

Peking University

92 PUBLICATIONS 673 CITATIONS

[SEE PROFILE](#)



Biao Wang

Sun Yat-Sen University

121 PUBLICATIONS 1,399 CITATIONS

[SEE PROFILE](#)

Some of the authors of this publication are also working on these related projects:



The magnetism studies for materials [View project](#)

All content following this page was uploaded by [Faxin Li](#) on 13 March 2014.

The user has requested enhancement of the downloaded file.

Estimation of the elasto-plastic properties of metallic materials from micro-hardness measurements

Chunyu Zhang · Faxin Li · Biao Wang

Received: 24 December 2012 / Accepted: 21 February 2013 / Published online: 5 March 2013
© Springer Science+Business Media New York 2013

Abstract Although hardness testing is a cost-effective and reliable technique to quickly estimate the overall mechanical properties of materials, hardness is not a fundamental mechanical parameter and it is rarely used in constitutive modeling or in engineering design. This work proposes a procedure to derive the elasto-plastic properties of metallic materials from the Vickers and the Knoop hardness measurements. Through dimensional analysis and finite-element simulations, relationships between hardness testing variables and mechanical parameters (Young's modulus, yield strength, and strain hardening exponent) are built up. An inverse procedure is developed to derive the mechanical parameters within the framework of genetic algorithm. The method is verified against two bulk steel materials and it is shown the derived stress–strain curves are in good accord with those measured by tensile tests. Then the method is successfully applied to measure the elasto-plastic properties of the pore walls of a metallic foam material. The present method can achieve a performance as good as those based on the instrumented indentation test and it is more readily accessible to the industry considering all the measurements can be performed on a cost-effective micro-hardness tester.

Introduction

As a cost effective and versatile technique, hardness testing has been widely used to quickly evaluate the overall mechanical properties of materials. However, hardness is not a fundamental mechanical parameter and it is rarely used in constitutive modeling or in engineering design. Although look-up tables have been compiled to estimate tensile strength from the hardness, this conversion is purely empirical and is only applicable to very limited materials. In order to estimate the constitutive behavior of materials from hardness measurements, a great amount of attempts have been made to correlate the hardness with the mechanical parameters, among which Tabor's work [1, 2] may be the most acceptable. For the hardness measurements using spherical indenters (for example, the Brinell hardness test), the hardness is related to the yield strength by [1, 2]

$$H = \frac{P}{A} = \alpha \sigma_0 \left(\beta \frac{a}{D} \right)^n \quad (1)$$

where P is the applied load, $A = \pi a^2$ is the projected contact area, a is the contact radius, D is the diameter of the indenter, $\alpha \approx 2.8$ and $\beta \approx 0.4$ for materials (most are metals) whose uniaxial stress–strain curve obeys the following power-law relation,

$$\sigma = \sigma_0 \varepsilon^n \quad (2)$$

Equation (1) thus enables extraction of the flow stress σ_0 and the strain hardening exponent n of metallic materials from a series of hardness measurements performed at different depths or loads. For the hardness measurements using sharp indenters (for example, the Vickers indenters or the Knoop indenters), Tabor found that the hardness is proportional to a characteristic uniaxial stress σ_r measured at a material-independent uniaxial strain $\varepsilon_r \approx 0.08$ [1],

C. Zhang (✉) · B. Wang
Sino-French Institute of Nuclear Engineering & Technology,
Sun Yat-Sen University, Guangdong 519082, Zhuhai, China
e-mail: zhangchy5@mail.sysu.edu.cn

F. Li
State Key Lab for Turbulence and Complex Systems, College
of Engineering, Peking University, Beijing 100871, China

$$H = C \cdot \sigma_r \quad (3)$$

Equation (3) thus enables extraction of a single point ($\varepsilon_r \approx 0.08$) in the uniaxial stress–strain curve of the material.

Therefore, Tabor's work provides a convenient way to estimate the constitutive parameters from hardness measurements. However, as an assumption of fully plastic deformation is taken in Tabor's work, Eqs. (1) and (3) are only satisfied in the strict absence of linear-elastic deformations [3]. For most metallic materials with finite yield strength, an overlapping of the elasto-plastic and the large-deformations contact regimes precludes the development of the fully-plastic response required by Tabor's relation. As a consequence, the domain governed by Tabor's relation was found to be rather limited [3, 4]. To find the general correlations between the hardness and the uniaxial mechanical properties covering both elasto-plastic and fully-plastic contact regimes, a comprehensive dimensional analysis as well as systematic finite-element simulations were performed and a best-fit relationship is proposed for spherical indentations [3]. It is thus feasible to extract the parameters E , σ_0 and n through a series of hardness measurements performed at different loads where the contact regime of the materials evolves from elasto-plasticity towards full-plasticity.

The most notable advantage of using the spherical indentation to deduce the mechanical properties is that only one indenter is required because of the extra length scale inherent in the indenter. However, the hardness measurement using a spherical indenter has several disadvantages. (i) It may cause damage to the specimen because a large load (or deep indentation) is required to generate a noticeable residual impression. (ii) It may not be suitable to probe the plastic properties of thin films due to the substrate effects [5]. (iii) It is extremely difficult to manufacture a diamond indenter which is of the perfect spherical shape. Adopting sharp indentations can alleviate these disadvantages but the duality problem exists in the mechanical property extractions [6–8]. Recently, Casals and Alcala [8] found that the intrinsic duality is related to the lack of measurement of the amount of pile-up or sinking-in. With a qualitative knowledge on the development of pile-up or sinking-in at the contact periphery gained through inspection of the residual imprints, it would be promising to extract the plastic properties from a single sharp indentation or extract the elasto-plastic properties from dual sharp indentations.

The main objective of this study is to devise a methodology to estimate the elasto-plastic properties of metallic materials from the hardness measurements using the two most frequently used sharp indenters, i.e., the Vickers indenter and the Knoop indenter. Starting from prior works

on dimensional analysis of sharp indentations [7], explicit expressions of the correlations between the hardness and the uniaxial mechanical properties are sought through extensive finite element simulations. An optimization procedure is proposed to derive the Young's modulus, the yield strength and the strain hardening exponent from a Vickers hardness measurement and a Knoop hardness measurement. The method is verified against two bulk steel materials and it is shown the overall stress–strain curves derived from the hardness tests are in good agreement with those measured by tensile tests. Then the method is successfully applied to measure the elasto-plastic properties of the cell walls of aluminum foams.

Relationships between hardness and mechanical properties

Dimensionless functional forms

Throughout the study, the Vickers hardness and the Knoop hardness are calculated according to the standard ASTM E384-08. For the Vickers hardness,

$$HV = \frac{2P \sin(\theta/2)}{d^2} \approx \frac{0.1891P}{d^2} \quad (4)$$

where P is the applied load (N), d is the average length of the diagonals of the residual impression (mm), $\theta = 136^\circ$ is the angle between opposite faces of the Vickers indenter. For the Knoop hardness,

$$HK \approx \frac{1.451P}{l^2} \quad (5)$$

where P is the applied load (N) and l is the length of the long diagonal of the residual impression (mm).

In this study, the uniaxial stress–strain relationship of the indented material is assumed to obey the Hollomon law [9],

$$\sigma = \begin{cases} E\varepsilon & \varepsilon \leq \sigma_{y0}/E \\ \sigma_{y0}(E/\sigma_0)^n \varepsilon^n & \varepsilon > \sigma_{y0}/E \end{cases} \quad (6)$$

where σ_{y0} is the initial yield strength. Dimensional analysis yields the following dimensionless functional forms relating the Vickers hardness, the Knoop hardness and the constitutive parameters [7, 8],

$$\frac{HV}{\sigma_{r1}} = \Pi_1 \left(\frac{E^*}{\sigma_{r1}}, n \right) \quad (7)$$

$$\frac{HK}{\sigma_{r2}} = \Pi_2 \left(\frac{E^*}{\sigma_{r1}}, n \right) \quad (8)$$

where the two uniaxial stresses, i.e., σ_{r1} and σ_{r2} , are defined at two characteristic strains, respectively. $E^* \equiv E/(1 - \nu^2)$ is the reduced modulus and ν is the Poisson's ratio.

At the contact periphery in Vickers hardness tests, development of pile-up or sinking-in (Fig. 1) is very common and it is deemed necessary to consider the amount of pile-up or sinking-in in order to eliminate the intrinsic duality in the mechanical property extraction from the Vickers indentations [8]. Similarly, an extra dimensionless functional form can be set to characterize the pile-up and the sinking-in phenomena in the Vickers hardness tests,

$$\frac{A_t}{A} = \Phi_1 \left(\frac{E^*}{\sigma_{r3}}, n \right) \quad (9)$$

For the Knoop hardness tests, although the ratio between the lengths of the two distinct diagonals of the residual impressions can be similarly defined to formulate an extra functional form, in practice this is not recommended considering it is difficult to accurately measure the length of the short diagonal.

Considering there are only three constitutive parameters (i.e., the Young's modulus, the yield strength and the strain hardening exponent) in the Hollomon law (Eq. 9), in principle it is possible to deduce the elasto-plastic properties by solving Eqs. (7–9), which can be formulated by conducting a Vickers hardness test and a Knoop hardness test. With a modern micro-hardness tester, the two indenters can be switched conveniently.

Explicit best-fit functions

To explicitly define the above dimensional scaling relationships, finite-element simulations were performed with an open-source finite element solver, Code-Aster [10]. The Vickers indenter and the Knoop indenter were assumed to be rigid. Figure 2 shows the three-dimensional finite-element mesh used to model the indented material. The meshing strategy has been tested to be a best compromise between the computing time and accuracy of the numerical results. Convergence studies were conducted and insensitivity of the results to the mesh is insured.

In the simulations, large strains and rotations were taken into account. Meanwhile, the frictionless contact conditions were assumed in all simulations. The indented solid is

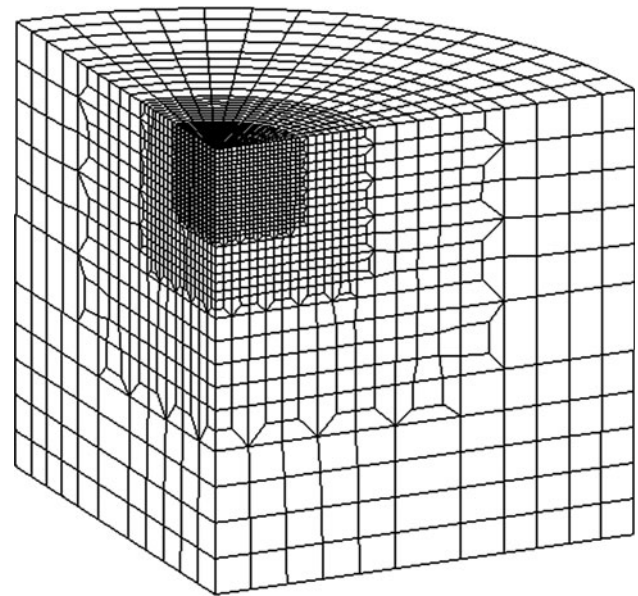
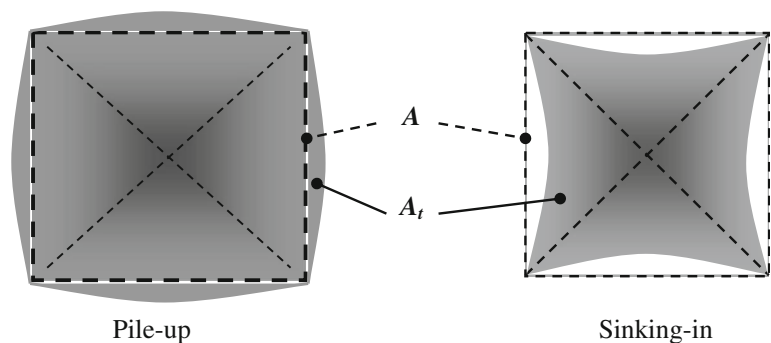


Fig. 2 Finite-element mesh used to model the indented material. Elements are refined in the potential contact region

assumed to obey the J_2 associative flow theory with the power-law strain hardening (i.e., Eq. 6). The mechanical parameters were generated by combining $E = 70, 110$, and 200 GPa; $\sigma_{y0} = 50, 100, 400$, and 1000 MPa; $n = 0, 0.1, 0.2, 0.4$, and 0.5 (where Poisson's ratio, ν , was fixed at 0.3). Totally 60 solids were indented with the Vickers tip and the Knoop tip, respectively.

The calculated Π_1, Π_2 and Φ_1 are, respectively, shown in Figs. 3, 4, and 5. On calculating Φ_1 , a planar surface covering the residual impression was firstly created by using a computer aided design software, i.e., SolidWorks, in order to evaluate the projected area of the residual impression. Early work by Tabor [1] and Chollacoop et al. [7] found that at a unique and material-independent characteristic strain ϵ_{r0} , the dependency of Π_1 or Π_2 on the strain hardening exponent vanishes. In this study, however, the characteristic stresses, i.e., σ_{r1} and σ_{r2} , should be defined at a strain away from this characteristic strain ϵ_{r0} in order to ensure a strong dependence on the strain hardening exponent in Π_1, Π_2 and Φ_1 . A total strain of 0.01 is

Fig. 1 Schematic representation of pile-up (*left*) and sinking-in (*right*) around the contact periphery of a Vickers indentation and the associated nomenclature. A is the nominal projected area and A_t is the true projected area



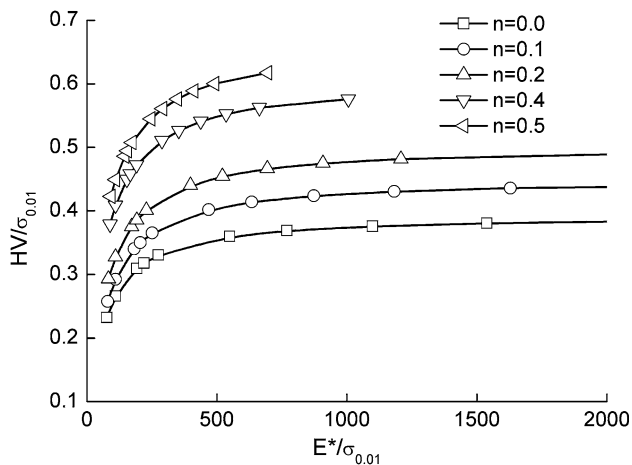


Fig. 3 Calculated Π_1 for the Vickers hardness

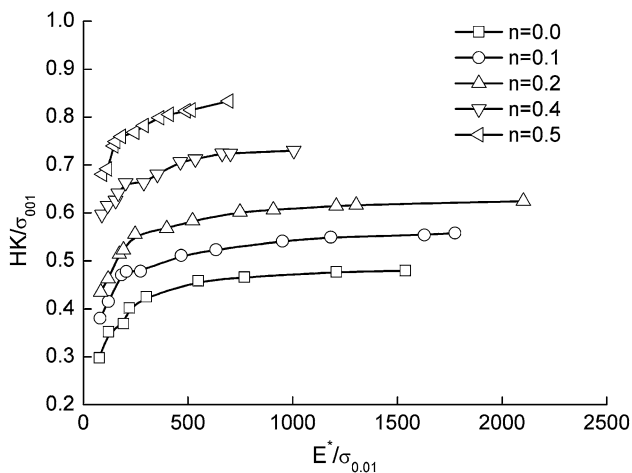


Fig. 4 Calculated Π_2 for the Knoop hardness

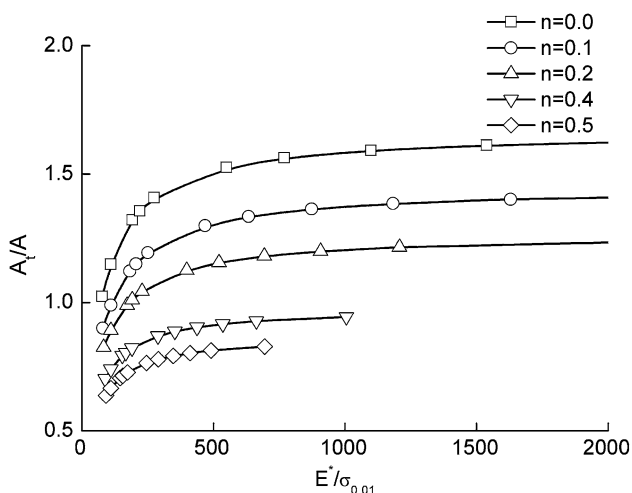


Fig. 5 Calculated Φ_1 for the Vickers indentation

recommended for both the Vickers indentation and the Knoop indentation. Both the dependency on n and the requirement of sufficient smoothness of the functions imply that $\varepsilon_{r1} = \varepsilon_{r2} = \varepsilon_{r3} = 0.01$ cannot be arbitrarily chosen.

By fitting the calculated Π_1 , Π_2 and Φ_1 , three explicit functions are recommended to represent the three dimensionless functional forms, i.e.,

$$\ln(HV/\sigma_{0.01}) = 0.4248 - 1.3406 \exp(-n) - 9.88174 \ln(E^*/\sigma_{0.01})/(E^*/\sigma_{0.01}) \quad (10)$$

$$HK/\sigma_{0.01} = 0.5372 - 0.26464n \cdot \ln(n) - 0.3850n/\ln(n)n - 2.0924/\sqrt{E^*/\sigma_{0.01}} \quad (11)$$

$$\ln(A_t/A) = -0.9858 + 1.4993 \cdot \exp(-n) - 8.3784 \ln(E^*/\sigma_{0.01})/(E^*/\sigma_{0.01}) \quad (12)$$

Mechanical property extraction from the hardness measurements

Once HV, HK and A_t/A are measured by hardness tests, the three mechanical parameters, i.e., E , σ_{y0} and n , can be deduced by solving Eqs. (10–12). In this study, the equations-solving problem is converted to an equivalent optimization problem, of which the objective function was defined as,

$$F(\mathbf{P}) = \left\| \frac{HV}{\sigma_{0.01}(\mathbf{P})} - \text{rhs}_1(\mathbf{P}) \right\| \cdot \left\| \frac{HK}{\sigma_{0.01}(\mathbf{P})} - \text{rhs}_2(\mathbf{P}) \right\| \cdot \left\| \frac{A_t}{A} - \text{rhs}_3(\mathbf{P}) \right\| \quad (13)$$

where $\mathbf{P} = (E, \sigma_{y0}, n)$ is the list of the three parameters to be identified; $\|\cdot\|$ represents the absolute value of a variable; rhs_1 , rhs_2 , and rhs_3 are the right-hand sides of Eqs. (10–12), respectively. Considering the advantage in achieving the global minima, the genetic algorithm is adopted to minimize the objective function until the prescribed criteria are satisfied.

To verify the method, numerical experiments were conducted. In the numerical experiments, HV, HK and A_t/A were collected from the finite element simulations conducted on five typical materials (Table I). The corresponding Π_1 , Π_2 and Φ_1 were then evaluated and passed to the genetic algorithm to finish the reverse analysis. The population size of the genetic algorithm was set to be 30 and each reverse analysis was repeated ten times. The evolution processes terminated when the value of the objective function was less than 10^{-5} . The mean values and the standard deviations of the extracted parameters are reported in Table 1. It is seen that all the three mechanical parameters, i.e., the Young's modulus, the yield strength and the strain hardening exponent, can be accurately derived by using the present method.

Table 1 A comparison of the extracted parameters with the exact parameters

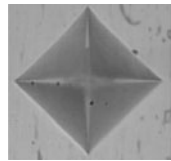
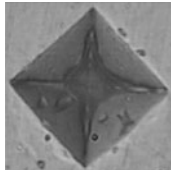
| Exact parameters | | | Identified parameters | | |
|------------------|---------------------|------|-------------------------------|--------------------------------|------------------------------|
| E (GPa) | σ_{y0} (MPa) | n | E (GPa) | σ_{y0} (MPa) | n |
| 210 | 500 | 0.1 | $210.1 \times (1 \pm 3.0 \%)$ | $499.9 \times (1 \pm 1.1 \%)$ | $0.1 \times (1 \pm 5.5 \%)$ |
| 210 | 1100 | 0.35 | $209.5 \times (1 \pm 2.5 \%)$ | $1098.8 \times (1 \pm 2.0 \%)$ | $0.35 \times (1 \pm 4.5 \%)$ |
| 210 | 220 | 0.2 | $210.0 \times (1 \pm 3.1 \%)$ | $220.0 \times (1 \pm 3.2 \%)$ | $0.20 \times (1 \pm 7.3 \%)$ |
| 70 | 500 | 0.12 | $70.1 \times (1 \pm 2.0 \%)$ | $500.1 \times (1 \pm 2.0 \%)$ | $0.12 \times (1 \pm 6.0 \%)$ |
| 110 | 830 | 0.15 | $110.0 \times (1 \pm 2.5 \%)$ | $830.0 \times (1 \pm 3.5 \%)$ | $0.15 \times (1 \pm 5.5 \%)$ |

Experimental verification and application

Two medium-carbon low-alloyed chrome-molybdenum martensitic steels were first tested and analyzed by the present method. The chemical composition of the first steel (S1) and the second steel (S2) in wt.% (balance Fe) are C 0.45, Cr 14.96, Ni 0.24, Si 0.43, Mn 0.44, S 0.017, P 0.018 and C 0.13, Cr 12.9, Ni 0.17, Si 0.31, Mn 0.24, S 0.003, P 0.023, respectively. Both steel alloys were heated for 60 min at 982 °C and then air cooled to room temperature. Then the steels were tempered at temperatures from 204 to 649 °C for 2 h. The experiments were performed on carefully polished surfaces with the roughness of 1 μm using a diamond Vickers indenter and a diamond Knoop indenter. The measured data are listed in Table 2 and similarly, the area A_t is calculated with assistance of the computer aided design software by creating a planar surface covering the residual impression. The extracted mechanical parameters of the materials are listed in Table 3 and the derived tensile curves are compared with the actual uniaxial tensile curves as shown in Fig. 6. It can be seen that the overall stress–strain curves derived from the hardness tests are in good accordance with those measured by tensile tests, which confirms the validity of the proposed method.

Considering the micro-hardness tests can be performed at a small scale as the instrumented indentations, the above established method is especially suitable to characterize the mechanical properties of materials with complex meso-structures such as metallic foams [11]. As typical porous materials, metallic foams offer significant performance gains in light, stiff structures, for efficient absorption of energy, for thermal management and perhaps for acoustic control and other more specialized applications [11]. The present method provides a quick approach to evaluate the mechanical properties of the pore walls (i.e., the solid matrix) which are indispensable to material design and material selection. The material used for the tests was a commercially available closed-cell aluminum foam with a density of 401.4 kg/m³ (AoShenTe metallic materials technology Co. Ltd, Shanghai, PR. China). The solid making

Table 2 Hardness test data of two steel materials

| Material | HV (MPa) | HK (MPa) | A/A_t | Impression shape |
|----------|----------------------------------|----------------------|---------|---|
| S1 | 738.2 Load:9.81N ^a | 1320.1 Load:9.81N | 0.9747 |  |
| S2 | 451.4 Load:1.96N | 563.8 Load:1.96N | 1.0174 |  |

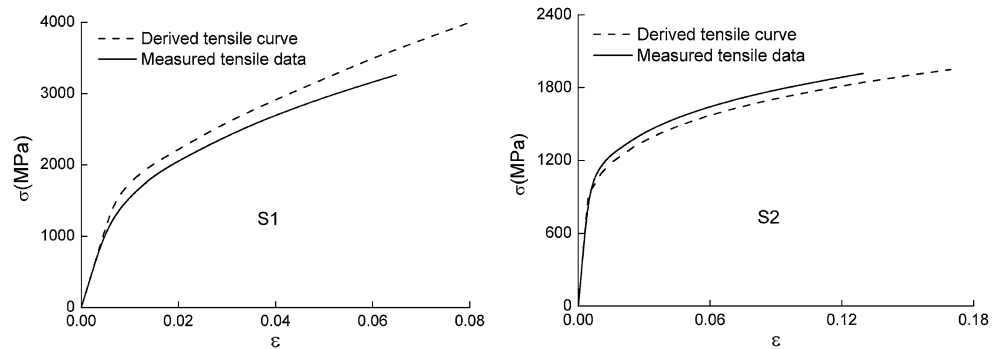
^a Load level adopted by the hardness measurements

up the foam is aluminum consisting of 0.6 % Mg as well as 0.5 % Si by wt. Three loads, i.e., 0.98N, 1.96N, and 2.94N, were applied in the Vickers hardness tests in order to check the influence of the indentation size on the derived mechanical parameters (Table 4). It is seen that the results derived from the hardness tests conducted at different loads are consistent with each other and all the extracted mechanical parameters are well within typical ranges of values.

It is worthwhile to note that although built upon the cost-effective non-instrumented indentation tests, the present method achieves a performance as good as those based on the instrumented indentation tests [6–8]. The reason lies in the intrinsic equivalence between the variables characterizing the instrumented and the non-instrumented indentations [8]. For example, the hardness measured in a non-instrumented indentation test is equivalent to the coefficient, say K , characterizing the loading segment of the load(P)–depth(h) curve of an instrumented sharp indentation test considering $P = K h^2$. Through dimensional analysis [8], it can also be shown that the parameter characterizing the pile-up and the sinking-in phenomena in the hardness test, i.e., A_t/A , is equivalent to the parameter characterizing the unrecoverable deformation

Table 3 Extracted mechanical parameters of two steel materials

| Material | E (GPa) | σ_{y0} (MPa) | n |
|----------|-------------------------------|--------------------------------|-------------------------------|
| S1 | $224.0 \times (1 \pm 3.3 \%)$ | $1370.1 \times (1 \pm 4.5 \%)$ | $0.407 \times (1 \pm 8.5 \%)$ |
| S2 | $202.8 \times (1 \pm 4.3 \%)$ | $921.1 \times (1 \pm 5.3 \%)$ | $0.207 \times (1 \pm 8.1 \%)$ |

Fig. 6 Comparison between the derived tensile curves and the measured uniaxial tensile curves**Table 4** Extracted mechanical parameters of the pore walls of the aluminum foam

| Load (N) | E (GPa) | σ_{y0} (MPa) | n |
|----------|------------------------------|-------------------------------|------------------------------|
| 0.98 | $72.0 \times (1 \pm 4.0 \%)$ | $193.1 \times (1 \pm 5.5 \%)$ | $0.26 \times (1 \pm 6.5 \%)$ |
| 1.96 | $74.8 \times (1 \pm 3.5 \%)$ | $196.7 \times (1 \pm 6.3 \%)$ | $0.26 \times (1 \pm 7.1 \%)$ |
| 2.94 | $73.5 \times (1 \pm 2.5 \%)$ | $192.9 \times (1 \pm 4.5 \%)$ | $0.26 \times (1 \pm 6.8 \%)$ |

A Poisson's ratio of 0.33 is assumed

in the instrumented indentation test, i.e., h_r/h_m , where h_r is the residual indentation depth and h_m is the maximum indentation depth.

Concluding remarks

A method to derive the elasto-plastic properties of metallic materials from the Vickers and the Knoop hardness measurements is developed in the study. Compared with the methods built upon instrumented indentations, the present method is more readily accessible to the industry considering all the measurements can be performed on a cost-effective micro-hardness tester. The validity of the method is ensured by the intrinsic equivalence between the variables characterizing the instrumented and the non-instrumented indentations. The accuracy of the method is demonstrated by the derived stress–strain curves which are in good accord with those measured by tensile tests. Although an extra measurement on the actual residual impression is needed, this step can be greatly simplified with assistance from image processing techniques.

Acknowledgements Financial supports from the National Natural Science Foundation of China (Grant No. 11002057) and from the National Basic Research Program (973) of China (Grant No. 2011CB606105) are gratefully acknowledged.

References

1. Tabor D (1951) Hardness of metals. Clarendon Press, Oxford
2. Hill R, Störakers B, Zdunek AB (1989) Proc Royal Soc Lond A 423:301
3. Alcalá J, Esqué-de los Ojos D (2010) Int J Solids Struct 47:2714
4. Mesarovic S, Fleck N (1999) Proc Royal Soc Lond A 455:2707
5. Zhang CY, Zhang YW (2004) J Mater Res 19:3053
6. Bucaille JL, Stauss S, Felder E, Michler J (2003) Acta Mater 51:1663
7. Chollacoop N, Dao M, Suresh S (2003) Acta Mater 51:3713
8. Casals O, Alcalá J (2005) Acta Mater 53:3545
9. Hollomon JH (1945) Trans Am Inst Mining Metall Eng 162:268
10. Code-Aster. <http://www.code-aster.org/>
11. Ashby MF, Evans AG, Fleck NA, Gibson LJ, Hutchinson JW, Wadley HNG (2000) Metal foams: a design guide. Butterworth-Heinemann Press, Oxford